

WiFind: Driver Fatigue Detection with Fine-Grained Wi-Fi Signal Features

Weijia Jia^{ID}, Senior Member, IEEE, Hongjian Peng^{ID}, Na Ruan, Member, IEEE,
Zhiqing Tang^{ID}, and Wei Zhao, Fellow, IEEE

Abstract—Driver fatigue is a leading factor in road accidents that can cause severe fatalities. Existing fatigue detection works focus on vision and electroencephalography (EEG) based means of detection. However, vision-based approaches suffer from view-blocking or vision distortion problems and EEG-based systems are intrusive, and the drivers have to use/wear the devices with inconvenience or additional costs. In our work, we propose a novel Wi-Fi signals based fatigue detection approach, called WiFind to overcome the drawbacks as associated with the current works. WiFind is simple and (wearable) device-free. It can detect the fatigue symptoms in the vehicle without relying on any visual image or video. By applying self-adaptive method, it can recognize the body features of drivers in multiple modes. It applies Hilbert-Huang transform (HHT) based pattern extract method results in accuracy increase in motion detection mode. WiFind can be easily deployed in a commodity Wi-Fi infrastructure, and we have evaluated its performance in real driving environments. The experimental results have shown that WiFind can achieve the recognition accuracy of 89.6 percent in a single driver scenario.

Index Terms—Driver fatigue detection, channel state information, wireless signal processing

1 INTRODUCTION

ACCORDING to World Health Organization, over 3400 people die every day, and tens of millions of people are injured or disabled in road traffic crashes every year [1]. Among the crashes, driver fatigue had been the first-class killer reason, especially for many truck drivers, who used to drive day and night to transform goods on time. According to the report of the Insurance Institute for Highway Safety, truckers who drive more than twelve hours were 86 percent more likely to be involved in a crash than those who drive less than eight hours. Even worse, truckers continuously driving more than five hours face twice risk than peers who drive one to five hours [2]. Traffic safety is the primary goal for both the drivers, pedestrians as well as the goods owners. To protect the safety of all the parties, an accurate monitor system, which can adaptively detect the driver fatigue in a device-free way, is in a pressing need.

Driver fatigue detection approaches have been studied for many years. There are two primary kind methods: driver-performance based method and driving behavior based method. Driver-performance based methods are the primary orientation of studies, and it can be divided into two main categories: vision-based detection and EEG-based

detection. Vision-based detection is sensitive to drivers surface features, relating to the eye and eyelid movements [3]. When the drivers wear a pair of sunglasses or drivers' driving postures are variable, the system cannot detect the eyes. For drivers, it is costly to install these systems with corresponding equipment, such as camera monitoring system. In EEG-based detection, users are required to wear specialized equipment, such as a hat [4], to monitor EEG during the whole period of driving. Nevertheless, the invasive device inherently brings the uncomfortable driving feeling, which may further deteriorate driver fatigue. Besides, install the systems are also costly.

In the foreseeable future, we consider Wi-Fi is the standard configuration for a vehicle. Leveraging the Wi-Fi signals without any specialized equipment has the advantage than those who work with various sensors in driver fatigue detection. In fact, Radio Frequency(RF)-based sensor research is hot for a long time. From visible light to RF signal, the researchers put a lot of efforts both in location and motion sensing. Especially, with the advantages of non-intrusion and device-free, Wi-Fi signals contribute to human activities recognition by the received signal strength(RSS)-based method [5] and the Channel State Information(CSI)-based method [6]. It had been proved that the RSS-based method is less sensitive than the CSI-based method which is fine-grained with plenty of sub-carriers [7]. Although a series of CSI based sense systems have been proposed, we cannot directly apply the previous work to driver fatigue detection due to lacking of easy and direct detecting methods to this prominent problem.

In our work, we study the driver fatigue features and the impact of driver fatigue body features on Wi-Fi signal, and verify the feasibility of detecting the fatigue by its effects on

- W. Jia is with the Centre of Data Science University of Macau, SAR Macau 999078, China. E-mail: jiawj@umac.mo.
- H. Peng, N. Ruan, and Z. Tang are with the Department of Computer Science and Engineering, Shanghai Jiao Tong University, Shanghai 200240, China. E-mail: {superphj, domain}@sjtu.edu.cn, naruhan@cs.sjtu.edu.cn.
- W. Zhao is with the American University of Sharjah, PO Box 26666, Sharjah 26666, UAE. E-mail: zhao8686@gmail.com.

Manuscript received 31 Aug. 2017; revised 16 May 2018; accepted 12 June 2018. Date of publication 25 June 2018; date of current version 29 May 2020. (Corresponding author: Na Ruan.)

Recommended for acceptance by H. Wang.

Digital Object Identifier no. 10.1109/TBDA.2018.2848969

Wi-Fi signals. We leverage the commercial off-the-shelf (COTS) Wi-Fi infrastructures to detect driver fatigue with WiFind. The design of WiFind is realized through detecting the features of driver fatigue, including that of facial features and body movement features. We will identify the typical/unique features via the CSI-based method.

There are two main challenges in driver fatigue detection using Wi-Fi signals. The first challenge is that how to detect driver fatigue wirelessly while fatigue is a subjective psychological feeling. We carefully select the corresponding features in driver fatigue scene. Based on the preliminary finding, We design and implement a self-adaptive method to turn WiFind into the corresponding mode to detect the fatigue features with targeted processing.

Another challenge is how to extract information in an efficient and targeted way. Raw CSI information includes lots of environment noisy, especially in the in-vehicle environment which is much narrower than an indoor environment. In the motion detection mode, based on our experiments in the real driving scenario, we found that the pre-processing phase has more impact on the final fatigue recognition than the indoor environment. We have compared the behave of the pre-processing methods, and decide to apply the Hilbert-Huang transform(HHT) [8] to increase the accuracy of WiFind. When there are no motions can be detected, we use breath detection mode to keep track driver performance. In the breath mode, we use Hampel-filter and smooth method on the top five sensitive sub-carriers to filter environment noise.

In this work, our contributions are:

- We analyze the features of driver fatigue and its impact on wireless signals. We examine the challenges of driver fatigue detection in the real driving environment, and carefully design the recognition features based on the preliminary findings.
- We take the first attempt to present a device-free fatigue detection system, WiFind. We design WiFind to prejudge the state of drivers by the Coefficient of Variation(CV) of Wi-Fi signals to detect the corresponding features depending on different strategy. We divide the fatigue detection process into two modes, breath mode and motion mode. Especially, in motion mode, we design the HHT-based pattern extract method to minimize the influence of environment.
- We implement WiFind with commercial hardware in real driving environments. The results show that WiFind can detect the driver fatigue with the total accuracy of 89.6 percent, along with an false positive rate(FPR) less than 10 percent in a single driver scenario. In the multi-passenger scenario, WiFind can detect the driver fatigue with the total accuracy of 73.9 percent. We also evaluate WiFind in different scenarios, the results show the WiFind is robust.

The remainder of this paper is organized as follows. In Section 2, we introduce the background of this work. In Section 3, we introduce the research motivation by exploring the correlation between driver fatigue and CSI. We present the detailed design in Section 4, which is followed by Evaluation, Discussion and Related work in Sections 5, 6 and 7, respectively. Finally, we give the conclusion and future work in Section 8.

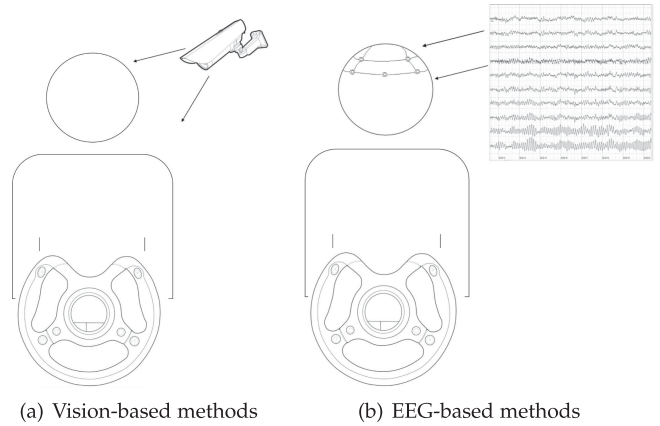


Fig. 1. Existing methods.

2 BACKGROUND

In this section, we introduce the scenario, the overview of the driver fatigue researches and the foundation of channel state information.

2.1 Scenario

During the corresponding transport high period, it is a typical situation that driver have to continuous working. We consider a scenario where a truck driver who is lack of sleep due to insomnia or carrying on night-shifting duty frequently. The driver driving along the highway for many hours, and feel drowsy with boring driving. Then the driver begins to feel heavy in the head, and get tired over the whole body. He or she give some yawns, then feels strained in the eyes. After several minutes, with the breath rate down he enters light sleep and intermittently nods. Finally, he or she unconsciously falls asleep on the steering wheel. Without alert in time, the truck is just like a monster running on the road ready creates dangerous for other cars and itself. We consider the Internet of Vehicles(IV) case in which a Wi-Fi hotspot can be set up in the car for communication and collaborative driving. Once the driver enters the cab, his mobile phone can connect to the in-vehicle Wi-Fi. With the help of our wireless sensing method, the driver's performance will be monitored during driving while the router continuous sends and receive the CSI and analyze them. Warning message will be sent to the driver's phone when the driver is detected with fatigue phenomena. In our work, we will show our approach will efficiently alert the driver fatigue.

2.2 Existing Methods

As shown in Fig. 1, existing work in driver fatigue detection with driver performance can be divided into vision-based methods and EEG-based methods based on the signal they use.

Vision-based methods deploy one video capture device close to the driver, which could be a camera. The camera will focus on the drivers' status and performance. When the driver begins to drive the car, the camera can monitor the driver's special features by checking the image of every frame and obtain suspected driver fatigue raw data. With the help of image algorithm, the vision-based system recognizes the real driver fatigue fragments. In the most of case,



Fig. 2. Driver fatigue detection with CSI of Wi-Fi.

the vision-based methods focus on only one kind of fatigue features. So they may fail in a specific case.

EEG-based methods monitor the electrical activity of the brain and focus on the 1–20 Hz band which corresponding to human's activities. This method deploys an EEG acquisition instrument on the driver' s head. The acquisition instrument was continuously collecting EEG signals for driver fatigue recognition. Compared with the vision-based methods, EEG-based methods directly try to explore the relationship between the human mind and EEG signals. But they are coarse-grained somehow because the signal they collect come from multi-zone of the brain. Signal analysis methods are widely used in EEG-based detection. In our opinion, the data collection process for EEG-based methods could be not comfortable for practical use. Besides EEG-based methods and vision-based methods are costly due to requirement of special equipments or devices.

Our work only uses simple Wi-Fi access points to collect the CSI signals when monitoring driver performance and detecting driver phenomena. As shown in Fig. 2, this method collects continuous CSI data in a non-invasive way and provide effective and cheap way to detect driver fatigue.

2.3 Wireless Communication

Wireless technology now is developing rapidly. Currently the modern commonly used high rate wireless communication technologies are the Multiple Input Multiple Output (MIMO) technology and the Orthogonal Frequency Division Multiplexing(OFDM) technology, and we briefly introduce them below.

MIMO is an emerging technology that is attracting wide attentions. It use multiple antennas and some coding technologies at the transmitter and the receiver. There are three main categories of coding technologies: precoding, spatial multiplexing and diversity coding. In a MIMO system, the transmitter and the receiver sends and receives multiple streams by multiple antennas. For each party, the signal Y received can be described as:

$$Y = HX + n,$$

where H is the channel matrix, and X and n are the original signal and noise, respectively. In the most of case, H is equivalent to CSI. Every element h_{ij} In H include an group of OFDM channel information.

The main idea behind the OFDM is to split the data stream to be transmitted into N streams of reduced data

rate and to transmit each of them on a separate sub-carrier. OFDM is similar to FDMA in that the multiple user access is achieved by subdividing the available bandwidth into multiple channels, which are then allocated to users. However, OFDM uses the spectrum much more efficiently by spacing the channels much closer together. This is achieved by making all the carriers orthogonal to one another, preventing interference between the closely spaced carriers. Therefore, spectral overlapping among sub-carriers is allowed, since the orthogonality will ensure that the receiver can separate the OFDM sub-carriers, and better spectral efficiency can be achieved than by using simple frequency division multiplex. In OFDM, each channel has a large number of orthogonal sub-carrier signals which maintain data rate equal to a single-carrier modulation scheme bandwidth. Compared to the single-carrier modulation scheme, OFDM has the advantage of robust when facing severe environmental condition. The communication link properties, such as scattering, fading, and power decay with distance will affect PHY layer information CSI.

2.4 CSI

In wireless communications, channel state information (CSI) refers to known channel properties of a communication link. This information describes how a signal propagates from the transmitter to the receiver and represents the combined effect of, for example, scattering, fading, and power decay with distance. The CSI makes it possible to adapt transmissions to current channel conditions, which is crucial for achieving reliable communication with high data rates in multi-antenna systems.

CSI needs to be estimated at the receiver and usually quantized and fed back to the transmitter (although reverse-link estimation is possible in TDD systems). Therefore, the transmitter and receiver can have different CSI. The CSI at the transmitter and the CSI at the receiver are sometimes referred to as CSIT and CSIR, respectively.

The CSI report field is used by the CSI frame to carry explicit channel state information to a transmit beamformer. The report field for 20 MHz has 56 CSI matrices for corresponding sub-carriers. Each matrix includes $N_r * N_t$ CSI streams, where N_r and N_t are the number of receive antenna and the number of transmit antenna. Each stream from a pair of receive antenna and transmit antenna include a group of OFDM channel state information elements. And each element in one stream includes the real part and the imaginary part. The time array of these elements are called sub-carriers which correspond to channels.

Since the received signal reflects the constructive and destructive interference of several multi-path signals scattered from the wall and surrounding objects, the movements of the driver while driving can generate a unique pattern in the time-series of CSI values, which can be used for driver fatigue recognition.

Researchers release the CSI tool for IEEE 802.11n measurement and experimentation platform. The CSI Tool is built on the Intel Wi-Fi Wireless Link 5300 802.11n MIMO radios, using a custom modified firmware and open source Linux wireless drivers. The IWL5300 provides 802.11n channel state information in a format that reports the channel matrices for 30 sub-carrier groups, which is about one

group for every 2 sub-carriers at 20 MHz or one in 4 at 40 MHz. Each channel matrix entry is a complex number, with signed 8-bit resolution each for the real and imaginary parts. It specifies the gain and phase of the signal path between a single transmit-receive antenna pair.

3 MOTIVATION

In this section, we illustrate the rationale behind CSI based driver fatigue signals using real-world experiment.

Before we experiment in driving scene, the first challenge is how to define driver fatigue exactly in a detectable way and how to measure it. Despite the huge progress of science in physiology and psychology, there is still no precise definition of fatigue. According to the medical observation, there is a relationship between fatigue and symptoms including body motions, temperature, skin electrical resistance, eye movement, breathing rate, heart rate, and brain activity. In some previous work [9], [10], researchers choose one or two symptoms to express fatigue activity because of the limitation of methods. In the same way, instead of defining fatigue, we choose some fatigue features to represent fatigue itself.

In the earlier fatigue studies, researchers try to find the relation between the fatigue and subjective symptoms by questionnaire survey [11]. They listed three groups symptoms which represent three fatigue factors: drowsiness and dullness, the difficulty of concentration and projection of physical impairment. The results show that the drowsiness and dullness factors have the highest frequencies than the other two factors. For both physical workers and mental workers, the drowsiness and dullness factors are the obvious symptoms during all day. The drowsiness and dullness factors include feel heavy in the head, get tired over the whole body, give a yawn, feel the brain hot or muddled, become drowsy, feel strained in the eyes, become rigid or clumsy in motion, feel unsteady in standing and want to lie down.

We reference the drowsiness and dullness factors and the typical driving scene which a truck driver drives alone along the highway in a night. In this scene, due to the lack of sleep and the boring driving, he feels sleepy and begins yawn. After several minutes, with the breath rate down he enters into light sleep and nod. Then he even asleep on the wheel. Therefore, how to effectively monitor and prevent driver fatigue has the extremely vital significance to reduce traffic accidents. Besides, with the help of vehicular communications [12] and fog computing to support mobility [13], it is possible to conduct such driver fatigue detection system inside the car. We try to use above typical features to represent driver fatigue and choose the following human body features:

Yawn. The meaning of yawn is not clear yet since lots of physiologists try to give different paraphrase vision. Yawning associated with a series of emotion state, and most often occurs during a fatiguing time. It consists of deep breathing, stretching of the upper body, opening mouth and covering mouth with hands.

Decrease of Breath Rate. Driver spirit state change to fatigue from awake couples with the decrease of breath rate at the start phase. Adults respiration usually has the frequency of 12-18 breath per minute [14]. When we breathe, our chest will have a expand and shrink because of inhalation and exhalation.

Nod. Unconsciousness nod which is one of the most dangerous motion for drivers often occurs light sleep phase. During nod, our head slowly down and sharp rise.

Sleep on the Steering Wheel. In some more worse cases, even the drivers bend over on the steering wheel. Note this is not the usual case in fatigue detection.

These features which represent driver fatigue all are time-phase activities, and the typical case has the common features and the possibility to be detected. Meanwhile, there are many confused drivers' motions which will also affect the CSI in the vehicle. We choose some of them: make a call, turn head, turn the steering wheel, start the car, and stop the car. We do not take these confused motions as fatigue motions. Because when the driver can make a call or turn the steering wheel, he is not fatigued.

We explore the driver fatigue impact on CSI in two cases. In the first case, the laptop is 5 meters from the router, and it sends ICMP packet every 300 milliseconds to router indoor. Then a person does above driver fatigue features on a chair and confused motions such as turn head, turn the wheel and make a phone call between the transmitter and receiver, about 2 meters away from the receiver. In the second case, we deploy devices on the front of a car. Then the driver behaves the same motions about 0.5 meters from the receiver while driving. From the laptop, we obtain the raw CSI data based on Orthogonal Frequency Division Multiplexing(OFDM) system in each process windows. Regarding communication theory, the capacity of a Multiple Input Multiple Output(MIMO) channels is $\min(m, n)$ times of a corresponding channel with a single antenna, where m and n are the numbers of antennas of receiver and transmitter. To get more information about CSI, we use MIMO technology for multiplying the capacity of a radio link using two antennas for transmitting and two antennas for receiving to form a 2×2 MIMO system to detect driving fatigue. As a result, the raw CSI data can be divided into 4 streams and has 30 sub-carriers in each stream. Then there are 120 groups of CSI data from each packet.

In Fig. 3, we plot the CSI sequences of one stream obtained during the two cases. The results present CSI varies over the time. The results show that the driver motions during driving are the major factors that cause the fluctuation of CSI waveform and shed light on detecting fatigue activities.

Fig. 3f presents how one of the confused activities affect CSI. We can find that the CSI sequences show different cycle when performing confusing activities. The change of CSI already can be recognized while the noisy signals are also strong. Besides in the data streams from a different group of transmit antenna and receive antenna, the CSI sequences presented the similar characteristic.

Above figure shows that the features we choose indeed can be recognized with CSI. Besides, the variation of CSI have some characteristics which need to be extracted with new method.

4 SYSTEM DESIGN

Fig. 4 presents the architecture of WiFind. First of all, the CSI is sampled in the same interval. In each interval, the self-adaptive mode will select the process mode, the motion detection mode or the breath detection mode. In the motion

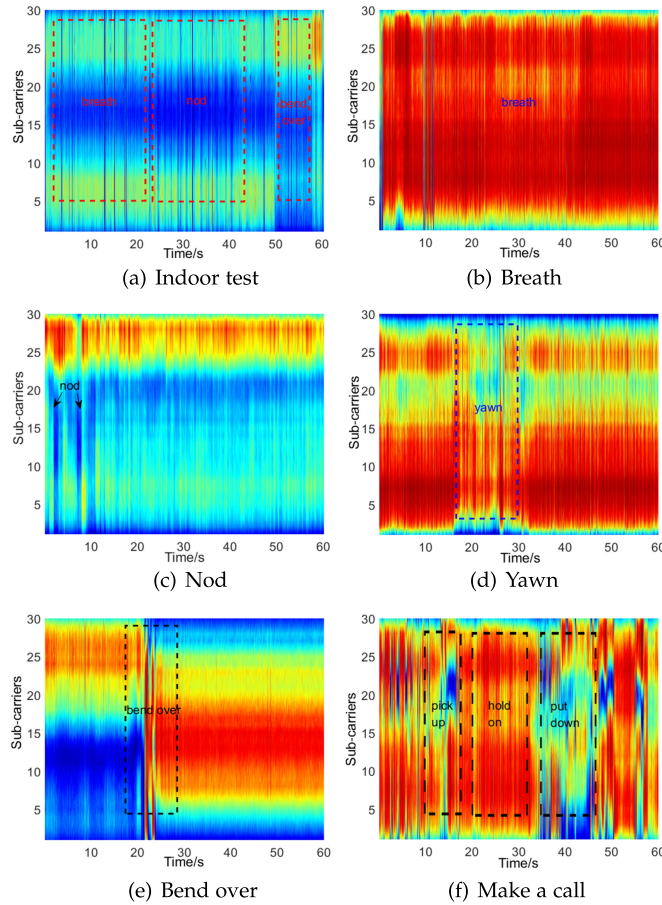


Fig. 3. The way driver fatigue affects CSI.

detection mode, we carefully extract the signal patterns with Hilbert-Huang transform and recognize driver fatigue with SVM method. When there are no driver's motions, we turn to breath detection mode. In the breath detection mode, we first filter and smooth the signals, then use the peak recognition method to get the drivers' breath rate for fatigue recognition.

Next, we elaborate the designs of WiFind relied on key function, such as data collection, self-adaptive mode, data pre-processing, pattern extraction, features extraction and recognition.

4.1 Data Collection and Self-Adaptive Mode

We collect CSI data during the driver driving on the real road by the receiver use the Internet Control Message Protocol(ICMP) get the transmitter's responses. And we find that different features impact CSI in different ways, but presented correlation with others. We find the characteristic of CSI as follow:

Sub-Carrier Sensitivity. In Figs. 3a, 3b, 3c, 3d, and 3e we plot the typical process of a human breath, nod, yawn and bend over indoor and in a vehicle, respectively. We can find the CSI sequences of a person on a chair or in a car presents strong correlation with human body features. These sub-carriers have different sensitivity. On one hand, 15-20 sub-carriers have less SNR in most of the case. On the another hand, for breath, nod, yawn all sub-carriers vary in a similar way which turns down while the motions happen. But bend over motion impact sub-carriers in another way that 5-20 sub-carriers SNR

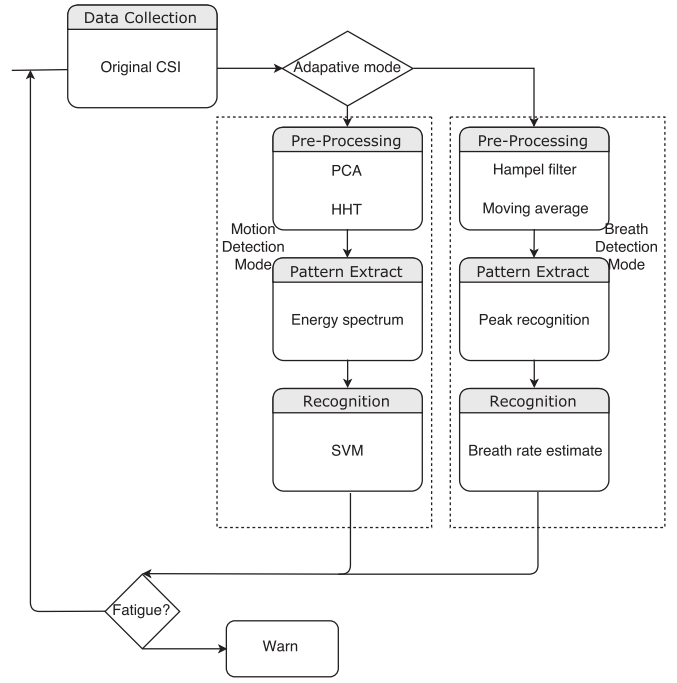


Fig. 4. Architecture of WiFind

rise whereas others turns down. Besides, the impact of yawn and nod on CSI cause more fluctuations. The reason behind these is that different frequency motions have the main impact channel region. The sub-carriers which mean the different channel state inherently have a unique law.

Sub-Carrier Correlation. The movements of head and hands result in correlated changes in the CSI sequences, and the sub-carriers that are closely spaced in frequency show similar variations whereas some sub-carriers that farther away in frequency show opposite changes. Despite the diversity of change, a strong correlation still exists, such as the 5-15 sub-carriers and the sub-carriers around 25 in Fig. 3d.

The Characters of Noise. From the raw CSI sequences, we can find the high-frequency noise full of the data stream, especially in the car scenario in Figs. 3b, 3c, 3d, 3e, and 3f. For different features, the impact of noise has an evident difference. The impact on the sequence of breath is larger than other motions because the displacement of the chest is not of the same magnitude with others.

Uncertainty. Actually, from Figs. 3a, 3b, 3c, 3d, 3e, and 3f we can notice the total CSI is entirely different with these signal come from different experiment and separate stream. We find even in the same car same driver behave same motion may result in a different variation of CSI. This characteristic keeps us from signal match methods, such as dynamic time wrapping(DWT), and turn us to the training methods.

According to the above findings, we find sub-carriers have different features in each case. Hence, how to de-noise, extract and leverage rich information for fatigue detection, from time-varying and regular CSI, needs detailed designs. We divide the system into two modes: motion detection mode and breath detection mode and use the basic and key function of WiFind, self-adaptive mode, to choose the corresponding mode. We will first judge whether the environment is relative 'stationary' which means there are no distinct human activities. This section relies on the observation of the top five

sensitive sub-carriers judgment. Here sensitive are defined by the coefficient of variation(CV) which can balance the difference caused by the environment. If CV value is less than the threshold value, WiFiFind will go to breath detection mode. Oppositely, it will go to the motion detection mode to detect corresponding motions. We set the process windows length to 20 seconds which longer than general human activities.

$$\sigma_{cv} = \frac{S}{M}. \quad (1)$$

S means standard deviation(STD), and M means the mean value(MEAN).

$$M = \begin{cases} M_m & \sigma_{cv} > \sigma \\ M_b & \sigma_{cv} < \sigma \end{cases}$$

Where M_m and M_b are the motion detection mode and breath detection mode, respectively.

4.2 Data Pre-Processing

For the motion detection mode, WiFiFind leverages sub-carriers correlation and calculates the principal components from all CSI time series by Principal Component Analysis(PCA). It then chooses the first principal components that represent the most common variations among all CSI time series. Notice sub-carriers in each TX-RX stream carry part of the information from motions impact, we will not devise a new sub-carriers select method. But the computational complexity of the method using all sub-carrier directly is unfriendly for further processing. PCA here reduces the dimensionality of the CSI information and removes noise by taking advantage of correlated variations of different sub-carriers.

Unlike in the indoor scene in the series of previous works, the motion detection environment is a narrow and noisy set. The methods based on the signal wave are invalid. We turn to the inherent characteristic and find that the key characteristic of the signal affected by the driver is the variation of the instantaneous frequency. There are two problems when we extract instantaneous frequency. First, in the traditional Fourier's analysis method, the frequency is defined in idealized infinite time sequence with constant sine or cosine waves. For the non-stationary time series, researchers developed the analysis methods with window-based methods, for instance, the Short-Time Fourier Transform(STFT) and Wavelet transform(WT). STFT method assumptions the signals are segment-wise stationary and neglects the instantaneous frequency of signals beyond or less than the window scale. WT methods have multi-resolution choose wavelet basis. But how to choose the wavelet basis relies on the researcher's experiences. The wavelet function has to be given before the analysis. These methods are all affected by uncertainty principle between time and frequency. Second, how to extract the instantaneous frequency uniquely needs detailed discussions.

In our work, we choose Empirical Mode Decomposition(EMD) and the Hilbert spectrum, which has been called HHT [8] together, to solve above problems. It had been applied in a series of signal process area, such as the earthquake detection, sound analysis. EMD method decomposes the non-stationary time series into several component functions, which are symmetric concerning the local zero mean, and have the same numbers of zero crossings and extremum. Researchers named

the oscillation mode imbedded in the data as Intrinsic Mode Function(IMF). We use the Algorithm 1 to self-adaptively decomposes signals into IMFs based on the signal inherent character rather than a predefined primary function like other previous methods did.

Algorithm 1. Calculate the IMF of signals

Input: CSI time series after PCA: $s(t) = \{s(1), \dots, s(K)\}$
Output: IMF series: IMF= $\{imf(1), \dots, imf(N)\}$

```

1: while s(t) is nonmonotonic function do
2:    $x(t) = s(t)$ 
3:   loop
4:     Find the local maximum values series of s:
       $s_{max} = \{s_{max}(1), \dots, s_{max}(M)\}$ 
5:     Find the local minimum values series of s:
       $s_{min} = \{s_{min}(1), \dots, s_{min}(N)\}$ 
6:     Find the zero crossing point series of s:
       $s_0 = \{s_0(1), \dots, s_0(O)\}$ 
7:     Use cubic spline function  $f(t)$  to fit  $s_{max}$ 
8:     Use cubic spline function  $g(t)$  to fit  $s_{min}$ 
9:      $d(t) = [f(t) + g(t)]/2$ 
10:    if  $|M + N - O| \leq 1$  and  $d(t) == 0$  then
11:      Break
12:    end if
13:     $s(t) = s(t) - d(t)$ 
14:  end loop
15:   $imf(i) = s(t)$ 
16:   $s(t) = x(t) - s(t)$ 
17: end while

```

The IMFs have the certain physical meaning of the high-low frequency. The outliers of these components include the part that affected by the drivers' motions. The reason that we don't directly use the outliers of IMFs is that we find the data still have high-frequency noise which affects all the sub-carriers come from the change after we get the principal components of CSI. Besides, the most of the outliers are the environment noise. If we set the threshold higher, we will neglect some motions such as the nod. Otherwise, we will confuse these motions with noise. Here we change to the total instantaneous frequency because the influence motions cause signals include noise and itself. We apply the Hilbert transform to each IMF component and computing the instantaneous frequency. For a non-stationary time series, $X(t)$, we can always have its Hilbert Transform, $\hat{X}(t)$ as the convolution of $X(t)$ with frequency $1/t$

$$X(\hat{t}) = \frac{1}{\pi} P \int_{-\infty}^{\infty} \frac{X(\tau)}{t - \tau} d\tau, \quad (2)$$

where P indicates the Cauchy principal value. With this definition, $X(t)$ and $\hat{X}(t)$ form the complex conjugate pair, so we can have an analytic signal, $Z(t)$, as

$$Z(t) = X(t) + i\hat{X}(t) = a(t)e^{i\theta(t)}, \quad (3)$$

in which

$$a(t) = [X^2(t) + (\hat{X}(t))^2]^{1/2}, \theta(t) = \arctan\left(\frac{\hat{X}(t)}{X(t)}\right), \quad (4)$$

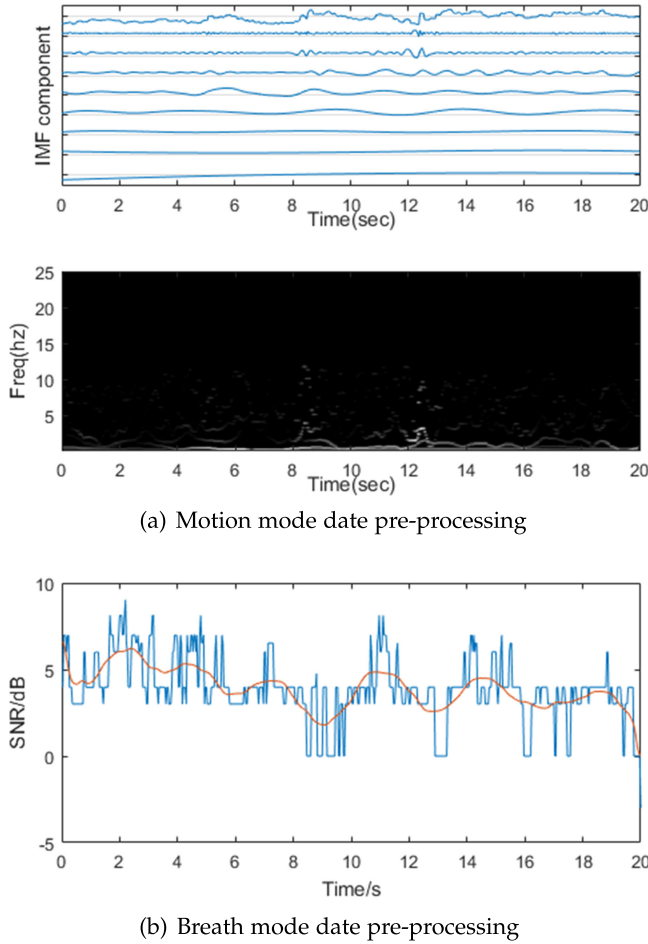


Fig. 5. Date pre-processing.

the instantaneous frequency is defined as

$$\omega = \frac{d\theta(t)}{dt}. \quad (5)$$

We can express the signals processed with performing the HHT on each IMF component as

$$\hat{X}(t) = \sum_{j=1}^n a_j(t) e^{i \int w_j(t) dt}. \quad (6)$$

Eq. (6) enables us to use a three-dimensional plot to represent the functions of amplitude and frequency and time. This plot is the Hilbert spectrum. Then we use the squared values of amplitude to produce Hilbert energy spectrum.

In the real driving scene, the breath detection is established with the assumption that the car is running on an ideal road which is long and smooth enough. The driver has no other motions during the detection intervals. This assumption corresponds to a 667m distance when the car run in 120 km/h in a process windows. This is common speed for a highway transportation. We continue to use the top five variance sub-carriers because they are sensitive to the breathing activity. To detect the breath rate in breath detection mode based on the above findings, the data stream of top five sensitive sub-carriers will first be applied with Hampel filter to remove significant outliers compared with neighbor measurements. Notice that these outliers will not confuse the motion detection because here we defined

the significant outliers as the CSI sequences whose frequency is less than 1 Hz.

In Figs. 5a and 5b, we notice the high-frequency noise in the car. It is observed that the frequencies of the variations in CSI time series due to breath lie between 0.25-0.3 Hz. So we next apply a moving average filter on the sequence to denoising. The ideal scene is uncommon in real driving. But the fatigued driving is uncommon concerning normal driving. Once the driver performs a motion, WiFiFind will change to motion detection mode which is common in daily life according to the adaptive mode.

4.3 Pattern Extraction

After we extract the HHT-based energy spectrum. We use the threshold value based method to extract the patterns that occur in driver motions. We sum the energy in time and compare it with the threshold. If the energy is greater than the threshold, it will be regarded as the start point of the driver motion. Next point whose energy less than the threshold will be regarded as the end point. Since the threshold is related to the environment, we set it with the average energy value of static environment as usual.

For the breath mode, we calculate the peak number to identify the frequency and use the Fake Peak Removal algorithm [15] to remove the peaks which are too close to others in the breath detection mode. Here we define the peak as the data sample that is larger than its two neighboring samples as usual. Then we filter the fake peak which is larger than two neighboring samples but smaller than most other samples or is very close to neighboring peaks.

4.4 Features Extraction and Fatigue Recognition

For the motion detection mode, from above steps, we obtain the data series, which is caused by different motions. Now it is important for us to extract the features that can stand for different motions from the data series. Based on the characters of the driver fatigue and the car scene, we choose the following features: (1) max total frequency energy, (2) mean of total frequency energy, (3) standard deviation (STD) of total frequency energy, (4) median absolute deviation(MAD) of total frequency energy, (5) length of the patterns extract from principal component, (6) mean of the pattern, (7) STD of the pattern, (8) MAD of the pattern.

As we have extracted the most representative features of different motions, we choose a correct classifier to recognize motions. In some previous researches, the Dynamic Time Warping method was used to compare the data series with the pre-defined standard gesture series. This method suits the situation that the equipment is in a fix indoor position. In our work, we apply the Support Vector Machine(SVM) to classify different motions.

In most of the cases, the data sets are not linearly separable in original space. Therefore, SVM method transforms the original space into a higher dimensional space to find a hyperplane which can discriminate the data sets by a good separation that has the largest distance to the nearest data point of any class. The SVM model can be formally described as:

$$\min_{w,b} \frac{\|w\|^2}{2}. \quad (7)$$



(a) Equipment



(b) Car

Fig. 6. Minimal WiFind setting.

Subject to $y_i(w^T \varphi(x_i) + b) \geq 1, i = 1, 2, \dots, n$, where x_i is the character of i th sample in higher dimensional space, y_i is the value of i th sample in higher dimensional space, $\varphi(x)$ is the kernel function and (w, b) is the hyperplane.

For linearly separable data, using Lagrange multipliers, we can attain the Lagrangian function as

$$L(w, b, \alpha) = \frac{1}{2} \|w\|^2 - \sum_{i=1}^n \alpha_i (y_i(w^T \varphi(x_i) + b) - 1). \quad (8)$$

Then, we put partial derivatives into Eq. (8) and get the Lagrangian conjugate function

$$L(w, b, \alpha) = \sum_{i=1}^n \alpha_i - \frac{1}{2} \sum_{i=1}^n \sum_{j=1}^n \alpha_i \alpha_j y_i y_j \varphi(x_i) \varphi(x_j). \quad (9)$$

It turns to optimization problem about α . Then we can obtain w, b

$$w = \sum_{i=1}^n \alpha_i y_i \varphi(x_i) \quad (10)$$

$$b = y_i - \sum_{j=1}^n \alpha_j y_j \varphi(x_j). \quad (11)$$

We use the w, b to construct the hyperplane to separate data by

$$f(x) = \text{sign}(w^T \varphi(x) + b). \quad (12)$$

In our work, we choose the radial basis function(RBF) kernel to accelerate the nonlinear relation with class labels and attributes. For performance and availability, we choose LIBSVM [16], an open source machine learning libraries to construct the classifier to recognize the motion is fatigued driving or not. This tool train a classifier for every pair of labels to extend the one class classification to multi-class classification.

For the breath detection mode, we notice the breathing activity is not a stable activity which has a fixed interval during driving. During each recognition windows, instead of estimating the fixed breathing circle, we directly sum the peak number up in each sub-carriers and achieve the breathing rate by using the following equation:

$$R = \frac{kT}{\sum_{j=1}^k N_j}. \quad (13)$$

Here T is the length of recognition windows, N_j is the peak number of the j th sub-carrier, and k is the number of the sub-carriers we select. Compared with the previous result, the decrease of breath rate which exceeds threshold will be judged into fatigue.



Fig. 7. Experiment path.

5 EVALUTION

5.1 System Setup

WiFind is built with the off-the-shelf hardware, which is a ThinkPad X200s laptop computer equipped with Intel Wi-Fi Link 5300 NIC, as shown in Fig. 6. The laptop runs Ubuntu 14.04 LTS with a modified Intel driver [6] to collect CSI data and is connected to a TP-LINK TL-WR842N wireless router which is used as a transmitter. WiFind serves as the receiver to request and receive the packets from the transmitter. Both devices operate in IEEE 802.11n mode at 2.4 GHz. To obtain the CSI data related to the driver's motions, WiFind sends ICMP packets with the sampling rate of 10 packets/s. In single driver scenario of this evaluation, the transmitter and receiver are placed in the front of driver's and co-pilot's seats, respectively. In multi-passenger and more complex path scenario, the transmitter and receiver are placed in the front of driver's seat and in the armrest box, respectively.

Before the experiment, we carefully studied the external influence on the Wi-Fi signal. Then we start the engine and turn on WiFind devices. In the first part of the test, a volunteer stands still on the side of the car. After dozens of seconds, he begins to walk around the car. The results are shown in Fig. 8. In another experiment, we pull over to the side of the road. In this experiment, several cars pass by, and we plot the WiFind measurement results in Fig. 9. We can notice that the in-car environment is similar to a closed indoor environment. The influence comes from the people or other vehicles outside the car is very slight. This experiment verifies our basic hypothesis and helps us to focus on the driver activities only.

We recruit 5 volunteers to join our evaluation, And the volunteers drive the corresponding routes following their own habits. As shown in Fig. 7, we choose two paths which can combine into a cycle. Every path includes many turn and crossing and speed bump. During the experiment, the volunteers participated in the data training phase and recognition phase by performing the specified actions. The examples of breath detection mode and motion detection mode are shown in Fig. 10 and Fig. 11, respectively. In the data training phase, at the marked location, volunteers complete corresponding fatigue features, and the camera in car record the happening time of fatigue behaves. Then WiFind records motions and its relevant CSI data. In the test phase, WiFind recognizes the motions or breath rate based on the observed CSI time series.

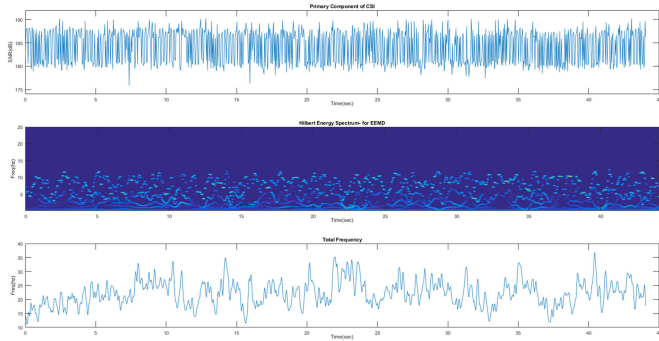


Fig. 8. Influence come from the people outside the car.

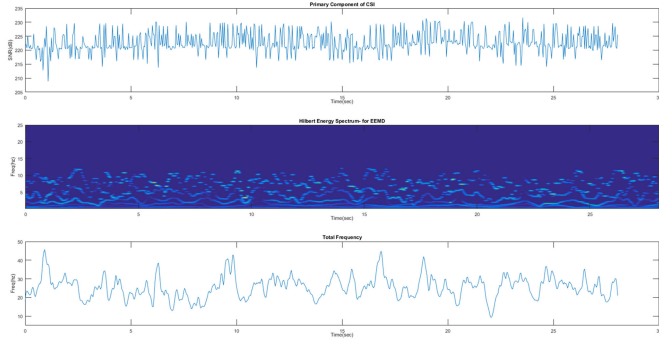


Fig. 9. Influence come from other cars outside the car.

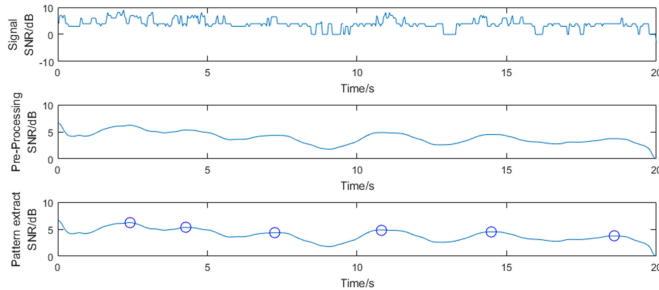


Fig. 10. Breath detection mode.

To quantify the performance of WiFind, we focus on (1) True Positive Rate (TPR): the fraction of cases where WiFind correctly detects the fatigue features among all the detected activities, (2) False Positive Rate (FPR): the fraction of cases where WiFind mistakenly recognizes fatigue when there is actually no fatigue motions. We start by evaluating the recognition accuracy in single driver scenario. Then we investigate various metrics that may influence the recognition accuracy of WiFind including the cars, people, and the paths. In the current stage of evaluation, we only focus on user-specific training. In Section 6, we will discuss the limitation of our method and its application in multi-passenger cases and explore the training influence for driver fatigue detection.

5.2 Accuracy of WiFind

In Section 3, we have shown that driver fatigue features may be correlated with different CSI waveforms. In this section, we aim to explore whether the differences of features are outstanding enough to be used for recognizing the different motions in the real-driving scenarios. We have collected the training and testing data from the 5 volunteers. Each

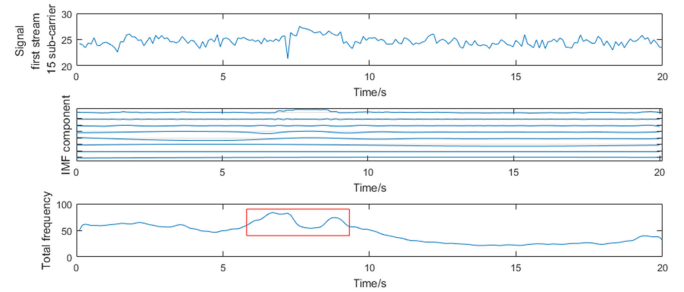


Fig. 11. Motion detection mode.

TABLE 1
Overall Accuracy of WiFind

	Breath mode	Motion mode
Ground truth	24	262
True Positive of WiFind	23	235
False Positive of WiFind	1	44
Total activities detected	67	837

volunteer first generates 5 loops of sampling features, where a loop is defined as the driving circle in which volunteers perform specific motions at fix location. After that, we evaluate the accuracy of WiFind through the collected CSI data. The accuracy is evaluated regarding cross-validation accuracy. In our problem setting, for every 5 loops dataset, we pick up one loop in turn for the testing data and choose the other 4 loops as the training dataset. WiFind adopts the recognition methods in Section 4 to recognize theses driver fatigue features. We evaluate CHANA EADO EV, BAIC MOTOR EV150, and TOYOTA PRADO. These cars travel at 40 km/h on the experiment paths. When we use all 5 loops data, WiFind achieves an average accuracy classification of 89.6 percent.

Table 1 presents the overall accuracy of WiFind in the real deployments. On the whole, WiFind successfully detects 89.6 percent of the fatigue activities and misjudges 6.6 percent of the usual activities.

In the case of motion mode, WiFind made some mistakes by confounding the nod motions with environment noise due to nod motion has the less duration than other activities. Also, the signal amplitude depends on the body type and habit of volunteers which make the node motion is hardly detected.

5.3 Impact of Different Configure

There are many factors potentially impacting the CSI. Even perform the same driver fatigue features, the different people, cars, and paths between AP and the mobile may also lead to a quite different CSI. We will investigate the impact of these configure on CSI in our experiments by comparing the accuracy of motion mode. Since motion detection mode is the main content of this paper, and breath mode uses the signal peak-based methods which are different with the motion mode. We will discuss it in Section 5.4. We plot the Receiver Operating Characteristic (ROC) curves of these setting in Fig. 12a. The ROC curve can depict the tradeoff between TPRs and FNRs over various settings.

5.3.1 Car

To compare the influence of the size of the car, we select the samples from TOYOTA PRADO, CHANA EADO EV, BAIC

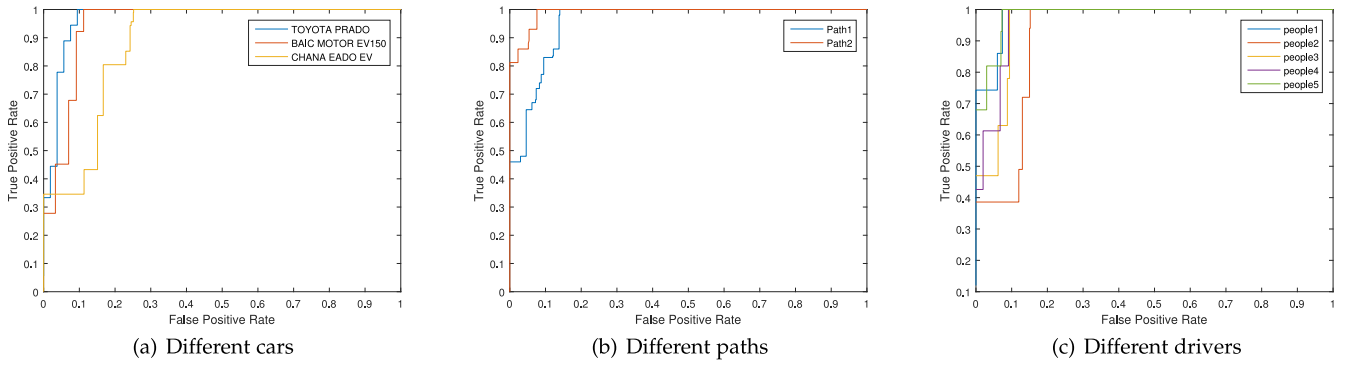


Fig. 12. ROC curves of different configurations.

MOTOR EV150 and CHANA EADO EV with the same drivers and the same path. The main difference of this samples' setting comes from the difference of automobile interior environment.

We find that the results of EV have poor performance in Fig. 12a, only provides a TPR less than 0.4 when the FPR is 0.1. The reason behind this result is that the information about driver motions have the strong correlation with space. PRADO and EV150 have relative large space between AP and receivers. It can identify 100 percent of the fatigue driving activities when FPR is 0.2.

5.3.2 Path

To compare the influence of the path, we select two samples which come from the same volunteer with the same car in different paths. To acquire the accuracy for these settings quantitatively, we plot the ROC curves of two paths in Fig. 12b. We found that driving along path2 has a poor influence on results. In path1 case, our method can identify more than 90 percent of the fatigue driving activities when FPR is 0.1 whereas path2 case provides 0.7 TPR when FPR is 0.1.

5.3.3 People

To compare the influence of different people, we plot the ROC curves of the five volunteers in Fig. 12c. We find that younger driver's sample(people2) corresponds to people5 has poor performance, only with TPR less than 0.4 when the FPR is 0.1. The reason behind this result is that every driver

has his own style in driving and younger driver's motions are much more unstable. The case of an experienced driver can identify all the fatigue driving activities when FPR is 0.1.

5.4 Robust of Breath Mode

Previous work on breath rate detection by using Wi-Fi [17] is in a quiet indoor environment. It will fail to detect one's breath rate when some users are moving around in the proximity. It's a big challenge to detect the driver's breath rate in a moving car. From another perspective, the breath detection is an auxiliary detection mode which will be active only when there are no motions detected. This challenge comes back to a moving static environment which is similar to an indoor scenario.

In our experiments in breath mode, we focus on the accuracy of detecting the decrease of breath rate instead of breath rate itself. The advantage of this method is that we minimize the driving environment influence in the same configuration by comparing the breath rate. This enables us to recognize nearly all the breath rate in the decreasing mode.

5.5 Compare with Baseline Methods

We compare WiFind with the method in the motion detection mode: Using outlier of the IMFs to detect the patterns [18]. Due to the features we detected differ from that used in vision-based or EEG-based methods, therefore, we will not compare our method with them directly. Instead of using the threshold value pattern extracted on energy spectrum, we select the third and the fourth IMF components which include the human activity frequency and use the outlier detection to extract the patterns.

To compare the overall identification accuracy of these methods quantitatively, we plot ROC curves of HHT and IMF outliers methods in Fig. 13. We found that using the outlier-based pattern extracting method has the poor performance, only provides TPR less than 0.8 when FPR is 0.05. The reason behind is that the patterns extracted include a huge amount of noise. Simply increasing the threshold of outliers will miss other minor motions, say the nod and turn head motions. This will result in FPR being declined and TPR increased. On the other hand, our HHT-based patterns extraction method can identify more than 80 percent of the fatigue driving activities when FPR is 0.05.

5.6 Impact of NLOS Propagation

We evaluate the performance of WiFind under the LOS, NLOS. In the NLOS case, the receiver is placed in the

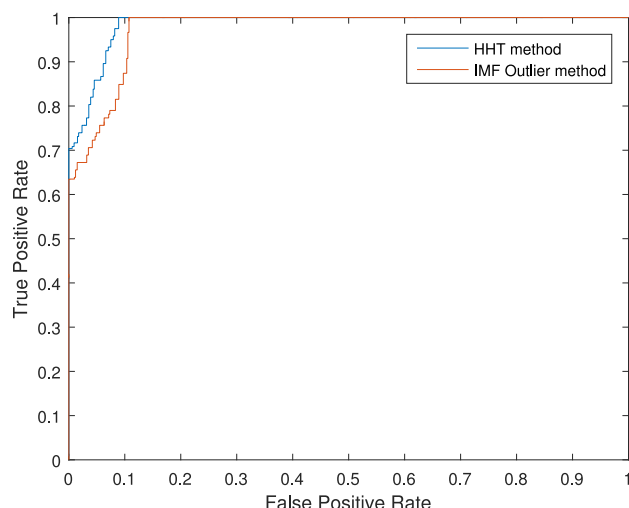


Fig. 13. ROC curves of methods.

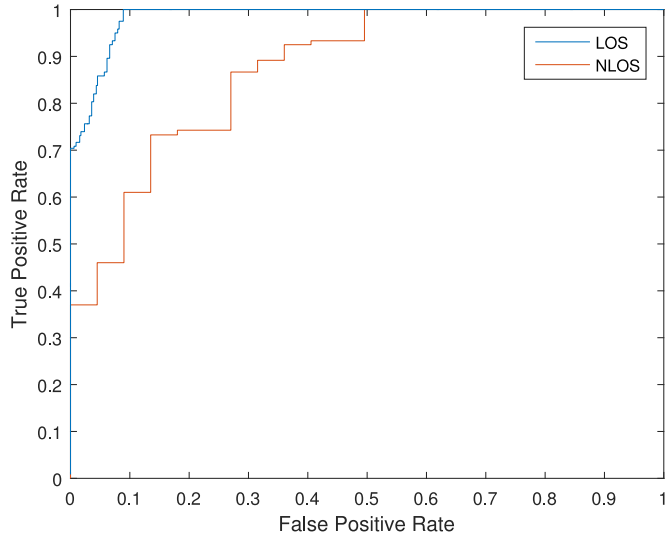


Fig. 14. ROC curves of LOS and NLOS.

backseat. We plot the Receiver Operating Characteristic (ROC) curves of the LOS and NLOS case in Fig. 14.

As expected, the accuracy degrades in NLOS scenario. When FPR is 0.1, TPR are less than 0.5 for NLOS. These results reveal that WiFind may not be ideal in NLOS scenario. Thus it works well for LOS case even with multi-passengers.

5.7 Multi-Passenger Case

Based on the method developed for a single driver, we now consider sensing driver fatigue in two persons' case, where the other person as the co-pilot. As the two persons can be viewed as two moving objects in the same driving environment, the total receiving signal variance can be approximated as a linear combination of the variance caused by the motions of each person. We cannot reference previous works on multi-user scene which usually split motions by their frequency. For usability of our method, we have to assume the impact of each person's motions influence to the receiving signal is independent and the motions from different persons may move at different time. We try to solve the reduced problem for multi-person case.

In the multi-person case, the two motions are collected as a single driver scene setting. Then we regard the co-pilots motions as the interference motions. For all motions include drivers fatigue features and normal motions and co-pilots all motions, we extract corresponding patterns, and use SVM to train the classifier. For the classification results, we sum them up according to label of driver fatigue.

Table 2 presents the accuracy of WiFind in multi-passenger case. On the whole, WiFind successfully detects 73.9 percent of the fatigue activities and misjudges 14.8 percent of the

TABLE 2
Accuracy of WiFind in Multi-Passenger Case

Motion mode	
Ground truth	188
True Positive of WiFind	139
False Positive of WiFind	64
Total activities detected	571



Fig. 15. More complex experiment paths.

normal activities. In this case, WiFind accuracy is influenced significantly by interference from co-pilot. But the result is kept at a useful level.

In fact, most of the wireless device-free activity sensing systems are designed for single person case. In the multi-person case, not only the other person's motions can affect the results, but also the variation of their position will change the sensing results. Considering these interference information need more calculation ability and other auxiliary devices which may betray our device-free original intention. Nevertheless, we consider WiFind is suitable for the transport trucks mostly with only one driver while the another person may have slept in the night.

5.8 More Complex Road Environment

To further evaluate WiFind, we conduct additional experiments with more complex and long-distance paths. The experiment paths are shown in Fig. 15. Our experimental environment includes a variety of road conditions, like toll highway, elevated road, and city road, etc. As shown in Fig. 15a, for the first complex experiment, we drive from Shanghai Jiao Tong University (SJTU) Minhang Campus, pass S4, S20, and G50 highway, arrive at Shanghai Hongqiao International Airport, and then return to SJTU on Jiamin Elevated Road and S4 highway during non-rush hour. The total path is 55.8 km long and takes 1 hour and 22 minutes. For the second complex experiment, as shown in Fig. 15b, we drive from SJTU, pass Hongmei South Road, Lingyun Road, Xinhua Road, and then arrive at Loushanguan Road during rush hour. The total path is 26.5 km long and takes 47 minutes. There are three people in the car: a driver, a co-pilot, and a passenger sitting in the back seat. For security reasons, the co-pilot simulates fatigue activities instead of the driver.

On the whole, WiFind successfully detects 594 total activities and 124 fatigue activities. For fatigue activities, there are 71 yawn activities, 45 nod activities, and 8 sleep on the steering wheel activities. WiFind totally detects 86 of all fatigue activities and the accuracy rate of fatigue detection is 69.35 percent, which is lower than the accuracy rate in 5.7. This is reasonable because the paths are more complex and there are many interference like the bumps on the road and the rotation of the head when the car turns. In short, we consider WiFind can still be used on the complex paths.

6 LIMITATIONS

In this section, we discuss the limitations of WiFind. WiFind's performance is achieved in an experimental environment. If

TABLE 3
True Positive Rate and Loop Times

Loop Times	One	Three	Four
True Positive Rate	73.2%	85.1%	89.6%

WiFind is applied in real environments, the following limitations must be considered:

Hardware Limitations. In WiFind, we use Intel 5300 NIC and Linux 802.11n CSI Tool [6]. In our experiments, even though we configure the ICMP request rate as 10 packets/s, the CSI collected are non-uniformly sampled and missing at some time. This problem is because of the influence of packet loss and transmission delay. For the motions happened in a short time, such as a nod, may entirely be neglected. On the other hand, the CSI is not the essential information in every packet yet. Now the standard request periodic measurement in wireless communication. Because compare with RSS, CSI takes up more space to describe every channel state. But as the importance of CSI in improving communication quality increase, and high rate wireless communication develops, CSI is replacing RSS as the essential information in every packet.

Fixed Setting. Currently, WiFind can only work for the situation that the drivers have fix driving habit such as the using hands when they yawn, and the AP and receiver need to be placed in a stable environment (This setting can be imagined as the central console with some advanced car-settings). But in reality, the driver may do the motions in a more free way (e.g., he may only open mouth when yawn or turn the wheel or other actions when yawn). Unfortunately, these are common problems in driving fatigue detection [19], [20]. This limitation can be overcome with continuous training similar to face recognition technology.

User Specific Training. Using WiFind, the driver's motions can be recognized via the classifiers trained from the same driver. In the real-world experiments, it is hard to adopt the classifiers trained directly in any drivers. This is because different people have different driving habits. A large number of training data based on a wide range of training samples may overcome this limitation. In practice, drivers need to participate training phase before they use WiFind to detect fatigue as initialization phase. Table 3 shows the true positive rate increases with the training loop increases. Even if there is only one training sample for one keystroke, WiFind can still achieve detecting rate 73.2 percent.

7 RELATED WORK

In this section, we review three domains of prior works that are tightly related to WiFind.

Vision-Based Methods. The vision-based fatigue detection methods have a long history. On the one hand, with the surveillance camera, researchers locate the face by using the features of skin colors [9], then detect the symptoms related to fatigue, such as the percentage of eye closure, eyelid distance changes with respect to the normal eyelid distance and eye closure rate in the method based on driver's state [10]. On the other hand, based on the driver's performance, researchers detect the head statement by the vision-based

method in which recognize the hair and head relation position to detect the nod or yawn phenomenon [19]. With the development of portable devices, smart glasses [21] and smartphones [22] also are used to do the fatigue monitoring.

EEG-Based Methods. Researchers are devoted to finding an effective indicator or developing accurate algorithms for EEG-based methods. From the statistical methods on all EEG bands [23], the mathematics combination of different bands [4], to focus on the index of one band, such as the alpha spindle [24] or Frobenius distance between 6 brain region of alpha band [25], most of the effect is put on the indicator selection of the EEG signals in recent years. Other researchers focus on the classification algorithm of EEG, such as the improved Support Vector Machine (SVM) [26] and independent component classification [27].

Wireless Signals. Researchers establish a series of motion [28] and gestures detection systems [7], [29] results in quite accurate detection. Pioneers release the modified wireless driver firmware to measure CSI based on the IEEE 802.11 standard in [6]. With the help of USRP software radios, WiSee was proposed for indoor gesture recognition [29]. WiHear is designed to focus the lip motion to identify the words they say [30]. To further explore human activity recognition, researchers in [31] recognizes human activity in the modeling and matching ways. Wifall uses the commercial Wi-Fi to detect the human fall [28]. WiKey gets the keystroke recognition by identifying the CSI pattern [32]. Smokey leverage rhythmical patterns of smoking impact the Wi-Fi signals to detect smoking [33]. In human respiration detection field, some researchers explore the Radio frequency method to recognize user breath rate [34], [35], [36]. The other researchers explore the propagation rule of Wi-Fi to understand and evaluate the human respiration detection in [15], [17].

8 CONCLUSION

We present WiFind, a device-free passive fatigue detection system that leverages the CSI variation information of Wi-Fi signals to detect the fatigue activity. We design a self-adaptive method to detect the breath and motions driver fatigue. We also elaborately leverage the common features to recognize the series of motions during fatigue. We prototype WiFind on commodity Wi-Fi devices and evaluate it in real driving environments. Experimental results show WiFind can achieve a recognition accuracy of 89.6 percent in a single driver scenario.

ACKNOWLEDGMENTS

This work is supported by FDCT/0007/2018/A1, DCT-MoST Joint-project No. (025/2015/AMJ) of SAR Macau; University of Macau Funds Nos: CPG2018-00032-FST & SRG2018-00111-FST; Chinese National Research Fund (NSFC) Key Project No. 61532013, NSFC No. 61702330, and National China 973 Project No. 2015CB352401.

REFERENCES

- [1] Violence and Injury Prevention. 2015. [Online]. Available: http://www.who.int/violence_injury_prevention/road_traffic/en/
- [2] Safety Defects and Long Hours Contribute to Large Truck Crashes. 2016. [Online]. Available: <http://www.iihs.org/iihs/sr/statusreport/article/51/10/4>

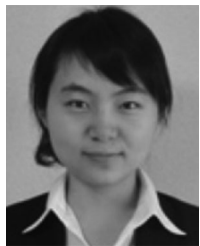
- [3] G. Sun, Y. Jin, Z. Li, F. Zhang, and L. Jia, "A vision-based head status judging algorithm for driving fatigue detection system," *Advances Transp. Stud.*, no. 37, pp. 51–64, 2015.
- [4] B. T. Jap, S. Lal, P. Fischer, and E. Bekiaris, "Using eeg spectral components to assess algorithms for detecting fatigue," *Expert Syst. Appl.*, vol. 36, no. 2, pp. 2352–2359, 2009.
- [5] P. Kumar, L. Reddy, and S. Varma, "Distance measurement and error estimation scheme for rssi based localization in wireless sensor networks," in *Proc. 5th IEEE Conf. Wireless Commun. Sensor Netw.*, 2009, pp. 1–4.
- [6] D. Halperin, W. Hu, A. Sheth, and D. Wetherall, "Tool release: Gathering 802.11 n traces with channel state information," *ACM SIGCOMM Comput. Commun. Rev.*, vol. 41, no. 1, pp. 53–53, 2011.
- [7] W. He, K. Wu, Y. Zou, and Z. Ming, "Wig: Wifi-based gesture recognition system," in *Proc. 24th Int. Conf. Comput. Commun. Netw.*, 2015, pp. 1–7.
- [8] N. E. Huang, Z. Shen, S. R. Long, M. C. Wu, H. H. Shih, Q. Zheng, N.-C. Yen, C. C. Tung, and H. H. Liu, "The empirical mode decomposition and the hilbert spectrum for nonlinear and non-stationary time series analysis," in *Proc. Roy. Soc. London A: Math. Physical Eng. Sci.*, vol. 454, no. 1971, 1998, pp. 903–995.
- [9] W.-B. Horng, C.-Y. Chen, Y. Chang, and C.-H. Fan, "Driver fatigue detection based on eye tracking and dynamk, template matching," in *Proc. IEEE Int. Conf. Netw. Sens. Control*, 2004, vol. 1, pp. 7–12.
- [10] Q. Wang, J. Yang, M. Ren, and Y. Zheng, "Driver fatigue detection: A survey," in *Proc. 6th World Congr. Intell. Control Autom.*, 2006, vol. 2, pp. 8587–8591.
- [11] H. Yoshitake, "Three characteristic patterns of subjective fatigue symptoms," *Ergonom.*, vol. 21, no. 3, pp. 231–233, 1978.
- [12] A. Zekri and W. Jia, "Heterogeneous vehicular communications: A comprehensive study," *Ad Hoc Netw.*, vol. 75, pp. 52–79, 2018.
- [13] Z. Tang, X. Zhou, F. Zhang, W. Jia, and W. Zhao, "Migration modeling and learning algorithms for containers in fog computing," *IEEE Trans. Serv. Comput.*, 2018, doi: [10.1109/TSC.2018.2827070](https://doi.org/10.1109/TSC.2018.2827070).
- [14] K. E. Barrett, et al., *Ganong's Review of Medical Physiology*, New York, NY, USA: McGraw-Hill, 2010.
- [15] J. Liu, Y. Wang, Y. Chen, J. Yang, X. Chen, and J. Cheng, "Tracking vital signs during sleep leveraging off-the-shelf WiFi," in *Proc. 16th ACM Int. Symp. Mobile Ad Hoc Netw. Comput.*, 2015, pp. 267–276.
- [16] C.-C. Chang and C.-J. Lin, "LIBSVM: A library for support vector machines," *ACM Trans. Intell. Syst. Technol.*, vol. 2, no. 3, 2011, Art. no. 27.
- [17] H. Wang, D. Zhang, J. Ma, Y. Wang, Y. Wang, D. Wu, T. Gu, and B. Xie, "Human respiration detection with commodity wifi devices: do user location and body orientation matter?" in *Proc. ACM Int. Joint Conf. Pervasive Ubiquitous Comput.*, 2016, pp. 25–36.
- [18] H. Peng and W. Jia, "Wifind: Driver fatigue detection with fine-grained wi-fi signal features," in *Proc. IEEE Global Commun. Conf.*, 2017, pp. 1–6.
- [19] M. Saradadevi and P. Bajaj, "Driver fatigue detection using mouth and yawning analysis," *Int. J. Comput. Sci. Netw. Security*, vol. 8, no. 6, pp. 183–188, 2008.
- [20] M. S. Devi and P. R. Bajaj, "Driver fatigue detection based on eye tracking," in *Proc. 1st IEEE Int. Conf. Emerging Trends Eng. Technol.*, 2008, pp. 649–652.
- [21] L.-B. Chen, W.-J. Chang, J.-P. Su, J.-Y. Ciou, Y.-J. Ciou, C.-C. Kuo, and K. S.-M. Li, "A wearable-glasses-based drowsiness-fatigue-detection system for improving road safety," in *Proc. IEEE 5th Global Conf. Consum. Electron.*, 2016, pp. 1–2.
- [22] Y. Qiao, K. Zeng, L. Xu, and X. Yin, "A smartphone-based driver fatigue detection using fusion of multiple real-time facial features," in *Proc. 13th IEEE Annu. Consum. Commun. Netw. Conf.*, 2016, pp. 230–235.
- [23] S. K. Lal, A. Craig, P. Boord, L. Kirkup, and H. Nguyen, "Development of an algorithm for an eeg-based driver fatigue countermeasure," *J. Safety Res.*, vol. 34, no. 3, pp. 321–328, 2003.
- [24] M. Simon, E. A. Schmidt, W. E. Kincses, M. Fritzsche, A. Bruns, C. Aufmuth, M. Bogdan, W. Rosenstiel, and M. Schrauf, "Eeg alpha spindle measures as indicators of driver fatigue under real traffic conditions," *Clinical Neurophysiology*, vol. 122, no. 6, pp. 1168–1178, 2011.
- [25] S. Charbonnier, R. N. Roy, S. Bonnet, and A. Campagne, "Eeg index for control operators mental fatigue monitoring using interactions between brain regions," *Expert Syst. Appl.*, vol. 52, pp. 91–98, 2016.
- [26] P. P. San, S. H. Ling, R. Chai, Y. Tran, A. Craig, and H. Nguyen, "Eeg-based driver fatigue detection using hybrid deep generic model," in *Proc. IEEE 38th Annu. Int. Conf. Eng. Med. Biol. Soc.*, 2016, pp. 800–803.
- [27] R. Chai, G. R. Naik, T. N. Nguyen, S. H. Ling, Y. Tran, A. Craig, and H. T. Nguyen, "Driver fatigue classification with independent component by entropy rate bound minimization analysis in an eeg-based system," *IEEE J. Biomed. Health Informat.*, vol. 21, no. 3, pp. 715–724, 2017.
- [28] Y. Wang, K. Wu, and L. M. Ni, "Wifall: Device-free fall detection by wireless networks," *IEEE Trans. Mobile Comput.*, vol. 16, no. 2, pp. 581–594, Feb. 2017.
- [29] Q. Pu, S. Gupta, S. Gollakota, and S. Patel, "Whole-home gesture recognition using wireless signals," in *Proc. 19th Annu. Int. Conf. Mobile Comput. Netw.*, 2013, pp. 27–38.
- [30] G. Wang, Y. Zou, Z. Zhou, K. Wu, and L. M. Ni, "We can hear you with Wi-Fi!" *IEEE Trans. Mobile Comput.*, vol. 15, no. 11, pp. 2907–2920, Nov. 2016.
- [31] W. Wang, A. X. Liu, M. Shahzad, K. Ling, and S. Lu, "Understanding and modeling of wifi signal based human activity recognition," in *Proc. 21st Annu. Int. Conf. Mobile Comput. Netw.*, 2015, pp. 65–76.
- [32] K. Ali, A. X. Liu, W. Wang, and M. Shahzad, "Keystroke recognition using WiFi signals," in *Proc. 21st Annu. Int. Conf. Mobile Comput. Netw.*, 2015, pp. 90–102.
- [33] X. Zheng, J. Wang, L. Shangguan, Z. Zhou, and Y. Liu, "Smokey: Ubiquitous smoking detection with commercial WiFi infrastructures," in *Proc. 35th Annu. IEEE Int. Conf. Comput. Commun.*, 2016, pp. 1–9.
- [34] H. Abdelnasser, K. A. Harras, and M. Youssef, "Ubibreathe: A ubiquitous non-invasive wifi-based breathing estimator," in *Proc. 16th ACM Int. Symp. Mobile Ad Hoc Netw. Comput.*, 2015, pp. 277–286.
- [35] F. Adib, H. Mao, Z. Kabelac, D. Katabi, and R. C. Miller, "Smart homes that monitor breathing and heart rate," in *Proc. 33rd Annu. ACM Conf. Human Factors Comput. Syst.*, 2015, pp. 837–846.
- [36] T. Rahman, A. T. Adams, R. V. Ravichandran, M. Zhang, S. N. Patel, J. A. Kientz, and T. Choudhury, "Dopplesleep: A contactless unobtrusive sleep sensing system using short-range doppler radar," in *Proc. ACM Int. Joint Conf. Pervasive Ubiquitous Comput.*, 2015, pp. 39–50.



Weijia Jia (SM'08) received the BSc and MSc degrees from Center South University, China, in 1982 and 1984, and the PhD degree from Polytechnic Faculty of Mons, Belgium, in 1993. He is currently taking leave from Shanghai Jiaotong University and joining University of Macau as chair professor. He is leading several large projects on next-generation Internet of Things, environmental sensing, smart cities and cyberspace sensing and associations etc. He has worked with German National Research Center for Information Science (GMD) from 1993 to 1995 as a research fellow. From 1995 to 2013, he worked in City University of Hong Kong as a full professor. He has published more than 400 papers in various IEEE transactions and prestige international conference proceedings. He is a senior member of the IEEE.



Hongjian Peng received the BA degree in logistic management from Dalian Maritime University, China, in 2014. He is currently working toward the master's degree in computer science and engineering at the Shanghai Jiaotong University. His research interests include Wireless sensor and big data.



Na Ruan (M'13) received the BS degree in information engineering, the MS degree in communication and information system from China University of Mining and Technology, in 2007 and 2009, respectively, and the DE degree from the Faculty of Engineering, Kyushu University, Japan, in 2012. Since 2013, she joined the Department of Computer Science and Engineering, Shanghai Jiaotong University as an assistant professor. Her current research interests include Wireless network security and game theory. She is a member of the Information Processing Society of Japan (IPSJ), China Computer Federation (CCF), ACM and the IEEE.



Zhiqing Tang received the BS degree from the School of Communication and Information Engineering, University of Electronic Science and Technology of China, China, in 2015. He is currently working towards the PhD degree in the Department of Computer Science and Engineering, Shanghai Jiao Tong University, China. His current research interests include fog computing, resource allocation, and reinforcement learning.



Wei Zhao (F'01) is currently with the American University of Sharjah, U.A.E. Before joining the the American University of Sharjah, he served as the rector of the University of Macau. He also served as the dean of the School of Science, Rensselaer Polytechnic Institute. Between 2005 and 2007, he served as the director of the Division of Computer and Network Systems in the US National Science Foundation when he was on leave from Texas A&M University, where he served as senior associate vice president for research and professor of computer science. As an elected IEEE fellow, he has made significant contributions in distributed computing, real-time systems, computer networks, cyber security, and cyber-physical systems.

▷ For more information on this or any other computing topic, please visit our Digital Library at www.computer.org/csl.